

## COOL STARS, THE SUN AND CLIMATE VARIABILITY: IS THERE A CONNECTION?

U. Cubasch<sup>1</sup>, E. Zorita<sup>2</sup>, J. F. Gonzalez-Rouco<sup>3</sup> and H. v. Storch<sup>2</sup>

<sup>1</sup>Meteorologisches Institut, Freie Universität Berlin, Carl-Heinrich-Becker-Weg 6-10, 12165 Berlin, Germany

<sup>2</sup>GKSS Research Centre, 21502 Geesthacht, Germany

<sup>3</sup>Dept de Astrofísica y Física de la Atmosfera, Universidad Complutense de Madrid, 28040 Madrid, Spain

### ABSTRACT

A simulation of the climate of the last millennium with a state-of-the-art ocean-atmosphere climate model, which has been forced with solar variability, volcanism and the change in anthropogenic greenhouse gases, shows global temperatures during the Little Ice Age of the order of 1 K colder than present, which is markedly colder than some accepted empirical reconstructions from proxy data. In this simulation temperature minima are reached in the Late Maunder Minimum, (around 1700 A.D.) and the Dalton Minimum (1820 A.D.), with global temperature about 1.2 K colder than today. The model also produces a Medieval Warm Period around 1100 A.D., with global temperatures approximately equal to present values.

Key words: solar variability and climate, Late Maunder Minimum, Medieval Warm Period, temperature reconstruction

### 1. THE CLIMATE SYSTEM

The climate system consists of the subsystems atmosphere, oceans (hydrosphere), the ice and snow cover (cryosphere), vegetation (biosphere), the land surfaces (pedosphere) as well as the lithosphere (cf., Fig. 1). The different climate sub-systems fluctuate at different time-scales. These different time-scales determine the time-dependent behaviour and represent therefore the dynamics of the climate system. Fluctuations in the climate system component at atmosphere, commonly called “weather”, vary at timescales from hours to days, deep sea currents and ice shields vary in time scales from centuries to millennia. As these climate components are interacting with each other, the variability of one sub-system influences the variability of the other sub-systems. In extreme cases it is therefore possible that a small disturbance is amplified by non-linear processes and has large impacts. The climate system is driven by external forcings. Here the prime forcing is the solar radiation, but also volcanism counts as external forcing for the climate scientists, as the aerosols emitted by the volcanoes modulate the incoming solar radiation. Mankind influences the climate system via the emission of greenhouse gases, pollutants and land usage. The solar forcing is only to a first approximation constant. Changes of the

orbit of the earth around the sun and variations in the solar radiative output represent a time dependent forcing. In this paper the response of the climate system to the temporal variability of the solar radiation, anthropogenic emission of greenhouse gases and volcanism is studied using a fully coupled ocean atmosphere model. This model is described in section 2, the experimental conditions are discussed in section 3. The model results are shown in sections 4 and 5, which is followed by a summary (section 6).

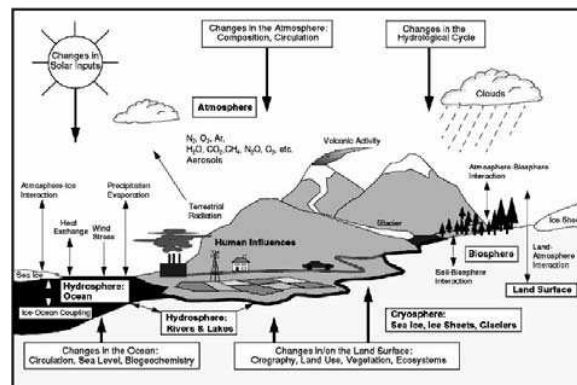


Figure 1. The climate system (IPCC, 2001)

### 2. THE MODEL

The climate model (ECHO-G) consists of the atmospheric model ECHAM4 with a horizontal resolution of  $3.75 \times 3.75$  degrees and 19 vertical levels, 5 of them located in the stratosphere, coupled to the ocean model HOPE-G with a horizontal resolution of approx.  $2.8 \times 2.8$  degrees with equator refinement and 20 vertical levels. The ocean and atmosphere models are coupled through flux adjustment to avoid climate drift in long climate simulations. This coupled model has been developed at the Max-Planck-Institute of Meteorology and it has been used in many studies of climate variability and climate change (Grötzner et al. 1998).

## 3. THE EXPERIMENT

For the simulation of the climate of the last 1000 years, the model was driven by estimations of past variations of the solar constant, volcanic activity and concentrations of greenhouse gases (derived from air bubbles trapped in polar ice cores (Etheridge et al. 1996, Blunier et al. 1995). Annual values of net radiative forcing due to solar variability and volcanic activity were estimated by Crowley 2000 from concentrations of  $^{10}\text{Be}$  (a cosmogenic isotope), from historical observations of sun spots and acidity measurements in ice cores. In this simulation, they were translated to variations in an effective solar constant communicated to the climate model, represented by a global annual number, equally distributed over the solar spectrum, with no seasonal or geographical dependence. In the last two centuries the solar component is very close to the Lean data (Lean et al. 1995). Changes in tropospheric sulphate aerosols and ozone concentrations have not been included.

## 4. RESULTS

The external climate forcing and the simulated global annual near-surface air temperature (SAT), is represented in Fig. 2. The model simulates a temperature maximum around 1100 A.D., the Medieval Warm Period (MWP) (Jones et al. 2001), with temperatures very similar to the ones simulated for the present period. The existence of the MWP has been recently a matter of considerable debate, since proxy data have not yielded a consistent picture of its existence (Bradley et al. 2001, Broecker 2001). In this simulation the MWP was a global phenomenon, probably caused by the maximum in solar activity in the 12th century. From 1300 A.D. global temperatures decrease and the simulation enters the so called Little Ice Ice (LIA) lasting until about 1850 A.D (Jones et al. 2001). Temperatures in the LIA were about 1 K colder than today's values, the cooling peaking in the Late Maunder Minimum (Eady 1976) (around 1700 A.D.) and the Dalton Minimum (Jones et al. 2001) (around 1820 A.D.), when simulated temperatures are about 0.25 K colder than the LIA mean. Subsequently, global temperatures start increasing almost continuously into the 20th century until the end of the simulation. The simulated secular warming trend in the 20th century is approached, but not surpassed, by warming trends around 1100 A.D. and in the 18th century (Fig. 2). A shorter simulation of the last 500 years with a slightly different model version yields similar results (Fig. 2).

The simulated temperature evolution is at variance with the most accepted empirical reconstruction (Mann et al. 1999). The empirical reconstructions based on different proxy data have targeted different temperatures, depending on the sensitivity of the proxies used. Thus, the multiproxy approach of Mann et al. (1999), hereafter MBH99, represents a reconstruction of the annual Northern Hemisphere (NH) temperature, whereas the reconstruction by Esper et al. (2002), based on extratropical dendrochronological data, is probably more strongly biased towards the NH extratropical summer temperatures. Instead of re-scaling the reconstruction to a common framework (Briffa and Osborn 2002), Fig. 3 shows these two not re-scaled reconstructions, together with the simulated NH annual temperature and the NH extratropical summer temperature. The discrepancies between reconstructions and simulations remain large, although up to 1600 A.D. the simulated values lie within the  $2\sigma$  errors of MBH99. The NH ECHO-G and MBH99 temperatures are reasonably correlated in the period 1000-1990 A.D., even when the long-term linear trends before and after 1900 A.D. are considered ( $r=0.25$  at interannual timescales,  $0.37$  at decadal and longer timescales), but the amplitude of the variations is clearly different. The ECHO simulations show a good agreement with a similar simulation of the last 500 hundred years, independently performed at the Hadley Center for Climate Research (Widman and Tett 2004). The latter

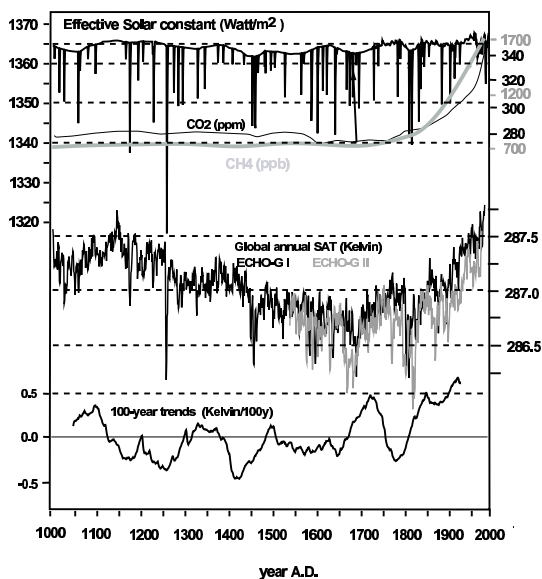


Figure 2. External forcing (effective solar constant and greenhouse gas concentration) used to drive the climate model ECHO-G; the simulated global annual surface air temperature (SAT) for two ECHO-G simulations and the running 100-year SAT trends for the 1000-year simulation. The spikes in the effective solar constant represent the effect of volcanic aerosols on the radiative forcing. In 1258-9 A.D. an eruption of unknown location, recorded in the acidity measurements of ice cores, causes a temperature drop of about 1 K.

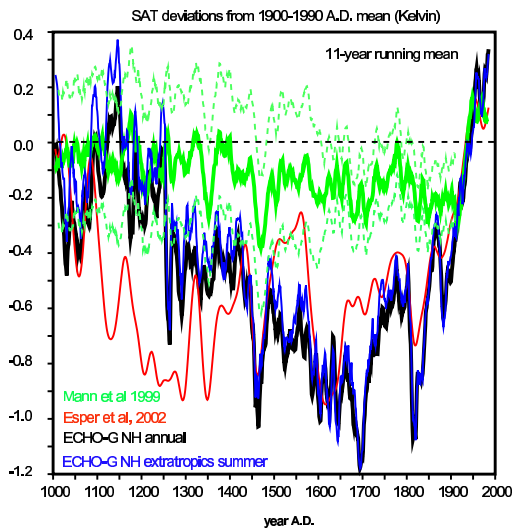


Figure 3. Simulated annual and summer extratropical North Hemisphere SAT deviations compared to two empirical reconstructions in the last millennium by Mann et al. (2000) and Esper et al. (2002).

model is not flux-adjusted, indicating that flux adjustment does not greatly distort the variability at long-time scales.

An assessment about the consistency of the model simulations and empirical reconstructions can be achieved by analysing the temperature evolutions in the 20th century, specially in the second half, when a global and complete climate data set of pseudo-observations- the National Centre for Environmental Prediction (NCEP) reanalysis (Kalnay et al. 1996) is available and solar output underwent strong variability (Lean et al. 1995). The analysis focusses on the NH temperature, which is arguably more reliable than the global mean. Fig. 4a shows the NH annual SAT from the NCEP reanalysis together with the evolution of the solar constant. The correspondence between both in the period 1948-1990 A.D. strongly suggests that the solar forcing contributed to a large extent to the North Hemisphere cooling between 1950 A.D. and 1975 A.D., the subsequent rapid warming (1975-1980 A.D.) and cooling (1980-1990 A.D.), a relationship also previously suggested from sea-surface-temperature data (White et al. 1997).

In the last decade greenhouse warming becomes dominant. The comparison with the (Jones et al. 1999) instrumental data set leads to a similar conclusion (Fig 4a). It is noted that ensemble simulations with the Hadley Centre model driven only by anthropogenic forcing deviate considerably from observations in this period (Stott et al. 2000). The inclusion of the effect of volcanic activity would

not have changed the overall picture, since in this period volcanic activity, as reflected in ice-core acidity measurements, was regularly distributed over time. The ECHO-G NH temperatures are depicted in Fig. 4b. Both show a similar evolution, ruling out internal variability as cause for this behaviour, and suggesting that the model is able to simulate reasonably the effects of a varying solar output. The solar signal in the NH NCEP temperature at 30 mb height (not shown) is not as clear and agrees better than in the simulations, but Fig. 4b also suggests that a complex stratosphere model may not always be required (Haig 1996), at least to simulate the NH temperature. Finally, Fig. 4c shows the MBH99 NH temperature, which in this period displays the smallest variability range.

## 5. CLIMATE SENSITIVITY

One can try to check the consistency of the different SAT data sets through a rough estimation of the sensitivity of the NH temperature to variations of the solar constant, although the climate sensitivity may be dependent on the previous pathway and mean state of the climate (Senior 2000; Meehl et al. 2002). By linearly detrending the temperature and solar constant in the 20th century, the presumably linear warming due to anthropogenic greenhouse gases and the linear increase in the solar constant may be filtered out. The correlation between detrended temperature and detrended solar constant should reflect the sensitivity of temperature to decadal variations of the solar constant, such as the ones of Fig. 4a. This correlation is represented in Fig. 5 for the NCEP reanalysis, the Jones et al. instrumental data, the longer ECHO-G simulation and the MBH99 reconstruction. The 20th century regression slopes yield a sensitivity of 0.13 K/(W/m<sup>2</sup>) for the NCEP and Jones et al. instrumental data set, 0.11 K/(W/m<sup>2</sup>) for ECHO-G temperature, and 0.08 K/(W/m<sup>2</sup>) for the MBH99 reconstruction. Previous estimations based on empirical reconstructions yielded a close value of 0.12 K/(W/m<sup>2</sup>) (Lean and Rind 1999). A value of 0.13 K/W/m<sup>2</sup> corresponds to a sensitivity to net radiative forcing of about 0.75 K/W/m<sup>2</sup>, assuming a fixed NH reflectivity of 30 %, which is closed to the assumed sensitivity to changes in greenhouse gas forcing (IPCC, 2001) and model simulations driven by solar changes (Cubasch et al. 1997). This sensitivity would explain about 0.2K of the NH warming in 1970-1999, approximately one third of the observed NH warming. This is close to a value of 40% estimated from simulations with other models driven by solar forcing alone (Cubasch et al. 1997).

The same sensitivity analysis has been carried out for the ECHO-G simulation and the MBH99 reconstruction in the period 1600-1900 A.D. In this period, greenhouse gases variations should have played a minor role, so that no other external trends are to be expected. This analysis yields a sensitivity of 0.16 K/(W/m<sup>2</sup>) for ECHO-G and 0.02 K/(W/m<sup>2</sup>) for MBH99. The data from this period

are also depicted in Fig. 5. The sensitivity of the ECHO-G model seems to have been larger in the previous centuries.

Uncertainties in this rough estimate, the different pathway and mean climate in the LIA (Senior and Mitchell 2000; Meehl et al. 2002), or the presence of stronger volcanic activity could contribute to explain this change. However, the sensitivity derived from the MBH99 reconstruction in the previous centuries is a factor 4 smaller than in the 20th century, possibly indicating that the reconstructions of the solar constant and the empirical temperature reconstructions in the previous centuries are not consistent with their behaviour in the 20th century.

## 6. SUMMARY

The discrepancies between model simulation and empirical reconstructions are discussed in terms of the climate sensitivity to changes in the solar constant. We find that whereas the model sensitivity is roughly constant along the simulation and agrees with the sensitivity derived from instrumental data, the empirical reconstructions show a lower sensitivity in the 20th century, and a much lower one in the past centuries, thus pointing to potential inconsistencies between the reconstructed temperature and solar constant.

## REFERENCES

- Blunier, T., Chappellaz, J.A. Schwander, J. Stauffer, B. & Raynaud, D., 1995, Variations in atmospheric methane concentration during the Holocene epoch, *Nature* 374, 46
- Bradley, S., Briffa, R.K. Crowley, T.J., Hughes, M.K. Jones, P.D. & Mann, M.E., 2001, *Science* 292, 2011
- Briffa, K.R. & Osborn, T.J., 2002, Blowing hot and cold, *Science* 295, 2227
- Broecker, W.S., 2001, Was the Medieval Warm Period Global? *Science* 291, 1497
- Crowley, T.J., 2000, Causes of climate change over the past 1000 years, *Science* 289, 270
- Cubasch, U., Hegerl, G.C., Voss, R., Waszkewitz, J. & Crowley, T.C., 1997, Simulation with an O-AGCM of the influence of variations of the solar constant on the global climate, *Clim. Dyn.* 13, 757
- Eady, J.A. The Maunder Minimum, 1976, *The Maunder Minimum*, *Science* 192, 1189
- Etheridge, D., Steele, L.P., Langenfelds, R.L., Francey, R.J., Barnola, J.M. & Morgan, V.I., 1996, Natural and anthropogenic changes in atmospheric  $CO_2$  over the last 1000 years from air in Antarctic ice and firn., 1996, *Geophys. Res.* 101, 4115
- Esper, J., Cok, E.R. & Schweingruber, F.H., 2002, Low-frequency signals in long tree-ring chronologies for reconstructing past temperature variability, *Science* 295, 2250
- Grötzer, A., Latif, M., Barnett, T.P.A., 1998, Decadal climate cycle in the North Atlantic Ocean as simulated by the ECHO coupled, *J. Clim* 11, 831
- Haig, D.H., 1996, The impact of solar variability on climate, *Science* 272, 981
- Houghton, J.T. et al., 2001, *Climate Change 2001: the scientific basis* (Cambridge Univ. Press, Cambridge, IPCC 2001)
- Jones, P.D., Osborn, T.J. & Briffa, K.R., 2001, The evolution of climate over the last millennium, *Science* 292, 662
- Jones, P.D., New, M., Parker, D.E., Martin, S. & Rigor I.G., 1999, Surface air temperature and its changes over the past 150 years, *Rev. Geophys.* 37, 173
- Kalnay, E. et al., 1996, The NCEP/NCAR 40-year Reanalysis Project, *Bull. Amer. Meteor. Soc.* 77, 437
- Lean, J., Beer, J. & Bradley, R., 1995, Reconstructions of solar irradiance since 1610-implications for climate change, *Geophys. Res. Lett.* 22, 3195
- Lean, J. & Rind, D., 1999, Evaluating su-climate relationships since the Little ice Age. *J. Atmos. Sol.-Terr. Phys.* 61, 25
- Mann, M.E., Bradley, R.S., & Hughes, M.K., 1999, Northern Hemisphere Temperatures During the Past Millennium: Inferences, Uncertainties, and Limitations, *Geophys. Res. Lett.*, 26, 759
- Meehl, G., Washington, W.M., Wigley, T.M.L., Alabaster, J. & Dai A., 2002, Solar and greenhouse gas forcing and climate response in the twentieth century, *J. Climate* 16, 426
- Senior, C.A. & Mitchell, J.F.B., 2000, The time-dependence of climate sensitivity, *Geophys. Res. Lett.* 27, 2685
- Stott, P.A., Tett, S.F.B., Jones, G.S., Allen, M.R., Mitchell, J.F.B. & Jenkins, G.J., 2000, External control of 20th century temperature variations by natural and anthropogenic forcings, *Science* 15, 233
- White, W.B., Lean, J., Cayan, D.R. & Dettinger, M.D., 1997, Response of global upper ocean temperature to changing solar irradiance, *J. Geophys. Res.* 102, 3255
- Widmann, M. & Tett, S.F.B., 2004, Simulating the climate of the Last Millennium. *IGBP Newsletter*, 56, 10

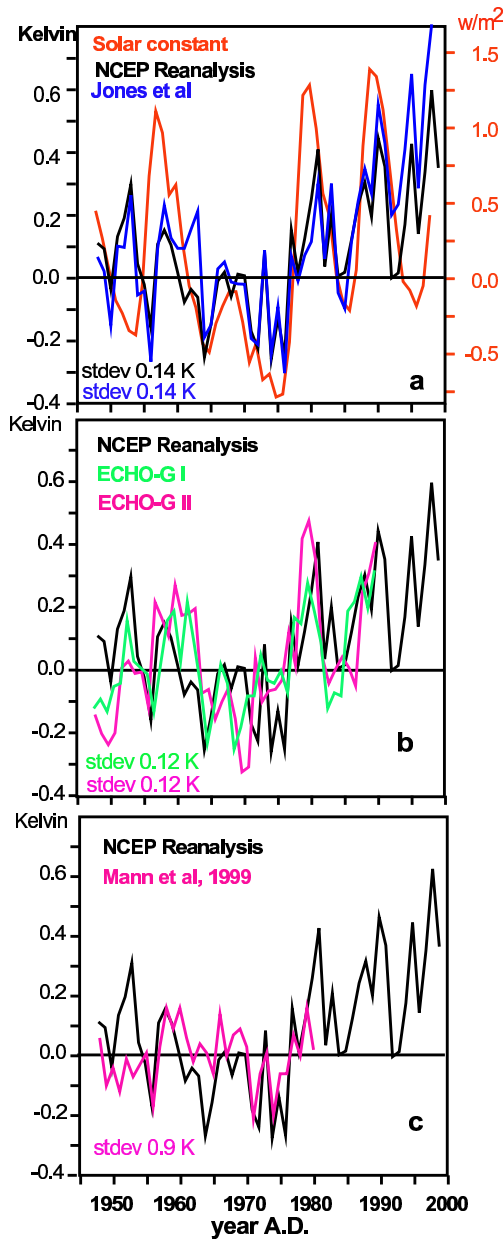


Figure 4. Comparison of different North Hemisphere surface temperature average in the period 1900-1999 from the NCEP Reanalysis, the ECHO-G simulations, the Jones et al. (1999) instrumental data set and the MBH99 reconstructions. The evolution of the solar constant as used in the ECHO simulations (derived from Crawford 2000) is also included in the upper-left panel. Data are deviations from the 1948-1980 mean.

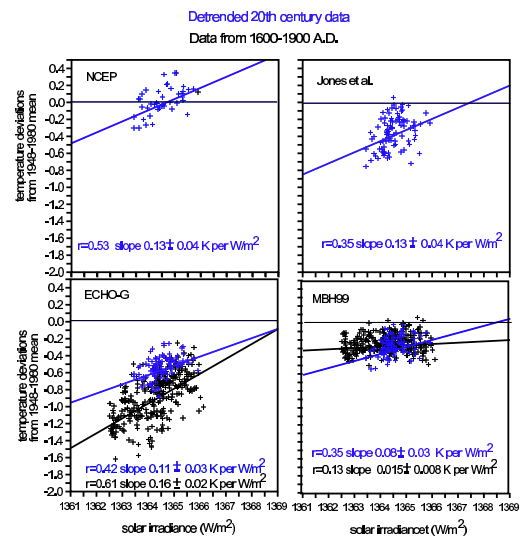


Figure 5. Scatter diagrams of annual solar constant, derived from Crawford (2000), and the North Hemisphere annual temperature deviations from the 1948-1990 mean for the NCEP data set, the Jones et al. (1999) instrumental data, the ECHO-G simulations and the MBH99 reconstruction. Black dots include data from the period 1600-1900 A.D., blue dots include linearly detrended data from 1900-1990 A.D. The correlation coefficients and the regression slopes are indicated.